Implementing a Triple L-shape Resonator on a Monopole Antenna for Multiband Operation in WLAN, WiMAX, 4G LTE, and 5G Sub-6G Networks

Vanvisa Chutchavong[1], **Wanchalerm Chanwattanapong**[1], **Thinnawat Jangjing**[2†], **Paitoon Rakluea**[2], **Norakamon Wongsin**[2], **Thanakarn Suangun**[3], **Chatree Mahatthanajatuphat**[4], **Nonchanutt Chudpooti**[5], and **Prayoot Akkaraekthalin**[4], Non-members

ABSTRACT

The present research proposes an innovative multi-band antenna design including a triple L-shape structure. This design is specifically targeted for utilization in a wireless local area network (WLAN), worldwide interoperability for microwave access (WiMAX), 4G LTE, and 5G Sub-6G networks. The antenna being considered is designed in an L-shaped layout, consisting of three separate components. The triple L-shape demonstrates the capacity to independently produce resonant frequencies. The middle L-shape, which is the longest, is notably responsible for generating the initial resonance frequency at 1.8 GHz. In addition, the L-shaped structure on the right exhibits a secondary resonance frequency of 2.45 GHz, whilst the L-shaped structure on the left generates a tertiary resonance frequency of 3.6 GHz. The proposed antenna demonstrates an extra resonance frequency of 4.6 GHz, which fits within the application frequency range of 5.2 GHz. The presence of the L-shape structure in the middle and right side of the suggested antenna arrangement is responsible for generating the 4^{th} resonance frequency, which can be attributed to the harmonic frequency. The antenna being discussed is fabricated on a FR4 substrate, measuring 30×50 mm^2 in size. After performing testing on the antenna, it is evident that both the simulation and measurement results demonstrate a suitable response across the whole operational frequency range. The antenna is capable of operating efficiently at specific frequencies. These frequencies include 1.8 GHz (1.71 GHz - 1.89 GHz) for LTE 1800, 2.45 GHz (2.39 GHz - 2.71 GHz) for IEEE 802.11b&g WLAN systems, LTE 2600, and 5G Sub-6G network, and 3.6 GHz (3.2 GHz - 5.37 GHz) for 5G Sub-6G network, WiMAX system, and IEEE 802.11a WLAN system. The success of this performance is demonstrated by the magnitude of the reflection coefficient, represented as $|S_{11}|$, which consistently stays below -10 dB. The antenna's average gain across all operational frequencies is approximately 2.5 dBi. Moreover, the antenna's radiation pattern maintains a consistent omnidirectional characteristic over the frequency bands of 1.8 GHz, 2.45 GHz, and 3.6 GHz. However, the radiation pattern at a frequency of 5.2 GHz displays distortion due to the antenna's higher-order mode. Furthermore, the antenna maintains its efficacy in wireless communication systems, such as devices that combine Wi-Fi and mobile cellular 4G&5G technologies in a single unit, occasionally called pocket Wi-Fi + 4G&5G cellular.

Manuscript received on October 27, 2024; revised on December 10, 2024; accepted on December 13, 2024. This paper was recommended by Associate Editor Kampol Woradit.

Keywords: Multiband, L-shape, WLAN, 5G networks

1. INTRODUCTION

The present-day phase of mobile phone communication technology is characterized by the emergence of 5G networks. Nevertheless, this technology is continuously evolving to meet the varied information retrieval needs of people in various fields, including education, health, and industry. The 5G sub-6G frequency band is commonly utilized due to its wide transmission range and minimal propagation loss. The proliferation of cellular coverage results in a decrease in the number of base stations. Consequently, there is a continuous advancement of antennas designed for mobile phones in the 5G sub-6G phase [1–5]. Moreover, various electronic devices, such as tablets, laptops, and GPS systems, require internet connectivity. To optimize user comfort, developers have designed a portable wireless gadget, popularly known as pocket Wi-Fi + cellular [6–9]. This device utilizes a

[1]The authors are with Department of Computer Engineering, School of Engineering, King Mongkut's Institute of Technology Ladkrabang, Bangkok 10520, Thailand.

[2]The authors are with Department of Electronics and Telecommunication Engineering, Faculty of Engineering, Rajamangala University of Technology Thanyaburi, Pathum Thani 12110, Thailand.

[3]The author is with Department of Electrical Engineering, Faculty of Engineering, University of Phayao, Muang Phayao, Phayao 56000, Thailand,

[4]The authors are with Department of Electrical and Computer Engineering, King Mongkut's University of Technology North Bangkok, Bangsue, Bangkok 10800, Thailand.

[5]The author is with 3Department of Industrial Physics and Medical Instrumentation, Faculty of Applied Science, King Mongkut's University of Technology North Bangkok, Bangsue, Bangkok 10800, Thailand.

[†]Corresponding author: thinnawat.j@en.rmutt.ac.th

Digital Object Identifier: 10.37936/ecti-eec.2525231.256482

cellular network to establish internet connectivity and then distributes the internet signals to various devices through the WLAN system. Hence, the utilization of multiband antennas holds great importance in the domain of wireless communication since they serve as the primary interface for these devices.

Several methods can be employed to develop an antenna capable of detecting a wide range of frequencies [10–14]. These methods include developing a wideband antenna with a frequency notch, utilizing the fractal concept in the design, and employing the multi-resonator method.

Drawing upon a comprehensive examination of previous literary investigations pertaining to the design of broadband antennas integrated with frequency notch techniques [15–19], this paper aims to enhance the antenna's responsiveness across multiple frequency bands. However, a disadvantage of this strategy is the inability to autonomously change the resonant frequency response. Moreover, the antenna's higher-order mode causes a modification in the radiation pattern as the frequency increases.

Researchers who looked at work on fractal multiband antennas [20–24] discovered that building the initial structure over and over again created more and more resonances, which led to a wide range of frequency responses. The process of creating a matching circuit for a fractal antenna that can handle many frequencies is quite difficult, requiring careful attention to detail in the overall design of the multi-frequency fractal antenna. Furthermore, its design exhibits a notable degree of intricacy, challenge, and difficulty. After examining the available literature on multiband antennas employing the multi-resonator approach [25–29], it is clear that this specific antenna structure consists of many resonators. Upon examination of the research, it was demonstrated that antennas possessing this specific configuration possess the capacity to detect and respond to a diverse range of frequencies. Moreover, it is possible to independently manipulate the generation of each frequency component based on individual preferences. Furthermore, the radiation pattern remains constant, showing minimal deviation in response to alterations in the fundamental frequency.

In order to support multiple operating frequency of 1.8 GHz, 2.45GHz, 3.6 GHz and 5.2 GHz and maintain the radiation patterns as omnidirectional for Pocket Wi-Fi application, this research presents an innovative multiband monopole antenna that utilizes a multi-resonator technique in its design. An important advantage of employing this technology is the antenna's capacity to autonomously regulate its frequency. The antenna being evaluated has been improved and perfected using the knowledge gained from prior multiband antenna designs indicated in the reference [30]. The suggested antenna development aims to build an antenna that can handle an increased operating frequency of 1.8 GHz within the 4G LTE system, surpassing its prior capabilities. Meanwhile, the applications that operate in the frequency bands of 2.4 GHz/5.2 GHz (as defined by the IEEE 802.11a/b/g WLAN standard), 3.5 GHz (utilized by WiMAX technology), and 2.6 GHz/3.5 GHz (linked to 5G technology) maintain their previous level of responsiveness. Moreover, the antenna being discussed consists of an L-shaped radiator that is separated into three equal halves. The center structure is precisely designed in an inverted L-shape form to achieve a resonance frequency of 1.8 GHz. The construction on the right-hand side has been precisely designed to provide a resonance frequency of 2.45 GHz. The structure in issue, which has an L-shaped form on the left-hand side, has been carefully designed to generate a resonance frequency of 3.6 GHz. Therefore, it is evident that all the proposed L-shaped configurations have an electrical length that is equal to one-fourth of the guided wavelength at various resonant frequencies. However, the antenna being discussed has been specifically designed for use on a generally available and cost-effective FR4-printed circuit board. A microstrip transmission line is used to connect the antenna to the SMA connector. In addition, the suggested antenna has been analysed to determine its many characteristics, such as the magnitude of the reflection coefficient $|S_{11}|$, gain, and radiation pattern. The investigation was performed with the CST Microwave Studio modeling software.

The presented document structure is organized in the following manner. The presentation of antenna design and analysis will be provided in Section 2. This part is comprised of two subsections, which will examine the investigation of the impacts resulting from altering different parameters. Additionally, an evaluation of the current distribution of the antenna will be conducted to analyze the noteworthy elements of the antenna design at the frequency of resonance. Subsequently, Section 3 will include the evaluation and elucidation of the diverse characteristics pertaining to the antenna under consideration. Additionally, the obtained measurements will be compared to the findings obtained from simulations. Subsequently, the last segment of the study will include the conclusion and subsequent analysis of the planned investigation.

2. ANTENNA DESIGN AND ANALYSIS

This section presents the antenna design recommended for use in pocket Wi-Fi devices since it is capable of supporting operating frequencies of 1.8 GHz, 2.45 GHz, 3.6 GHz, and 5.25 GHz. The proposed antenna is constructed using a FR4 substrate, which has a dielectric constant (ϵ_r) of 4.3, a loss tangent of 0.019, and a thickness of 0.8 mm. The proposed antenna is a monopole antenna that incorporates a multi-resonator radiator or triple L-shape radiator in order to achieve a broad frequency range. The frequency of 1.8 GHz is intentionally chosen to align with the physical lengths L_1 and L_2, ensuring that their combined electrical length is about a quarter of the guide wavelength ($\lambda_g/4$). At a frequency of 2.45 GHz, the aforementioned corresponds to the parameters L_3 and L_4,

***Table 1**: The proposed antenna's parameter summary.*

Parameter	Size (mm)	Parameter	Size (mm)
L	50	W	30
L_1	26	W_1	1.5
L_2	12.75	W_2	1
L_3	12	W_3	7.75
L_4	12.5	W_4	1.75
L_5	13	W_5	2.5
L_g	15.5	W_f	1.5
S_1	0.5	T_1	5
S_2	2.5	T_2	9
S_3	3	t_k	0.035
g	1	h	0.8

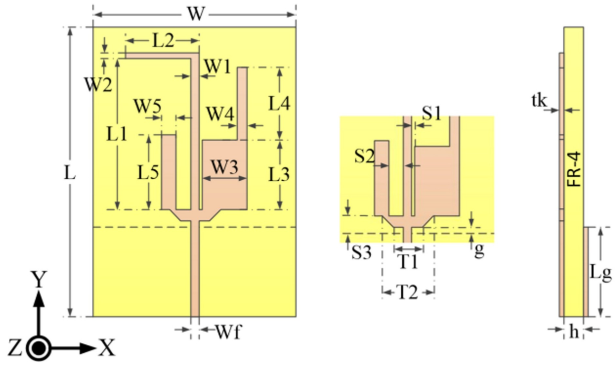

***Fig. 1**: The proposed antenna configuration.*

which possess an electrical length of about a quarter of the wavelength. The length L_5 is specifically designed to have an electrical length of about a quarter of the guide wavelength ($\lambda_g/4$) in order to achieve a frequency response of 3.6 GHz. However, it is worth noting that the operating frequency of 5.25 GHz corresponds to the harmonic frequency resulting from the specifications of L_2 and L_4, and it also exhibits an electrical length compatible with the parameters of L_3. Consequently, the antenna height at each resonant frequency can be determined using (1) to (3).

$$L_1 = \frac{c}{\left(4 f_{1.8GHz} \sqrt{\frac{\varepsilon_r + 1}{2}}\right)} \tag{1}$$

$$0.5L_3 + L_4 = \frac{c}{\left(4 f_{2.45GHz} \sqrt{\frac{\varepsilon_r + 1}{2}}\right)} \tag{2}$$

$$L_5 = \frac{c}{\left(4 f_{3.5GHz} \sqrt{\frac{\varepsilon_r + 1}{2}}\right)} \tag{3}$$

Furthermore, the multiband monopole antenna under consideration is fed by a microstrip transmission line with an impedance of around 50Ω. The transmission line is linked with a 50 Ω SMA connection. The proposed antenna dimension is about 30×50 mm^2. The diagram illustrating the configuration of the antenna under consideration is shown in Fig. 1. Consequently, the basic design specifications may be briefly stated in Table 1. The following section will examine the impact of altering several characteristics of the proposed antenna on frequency impacts.

2.1 Parameters Study

This research aims to examine the impact of resonance frequency on a system when there is a substantial change in parameters, namely L_2, L_4, L_5, L_3, and g. When investigating the impact of changes in the frequency characteristics of $|S_{11}|$ due to variations in the L_2 parameter, in accordance with the findings shown in Fig. 2. The reduction in the L_2 parameter is seen to result

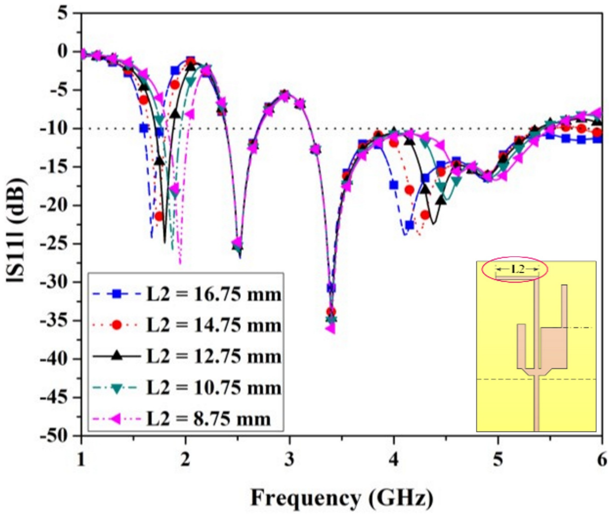

***Fig. 2**: The simulation result of the $|S_{11}|$ as varying the parameter L_2.*

in an upward shift of the resonance frequencies of the 1st and 4th towards higher frequencies. Simultaneously, the second and third resonant frequencies remain unaltered. The obtained findings demonstrate that the L_2 parameter has a notable influence on the resonant frequencies at the first and fourthmodes. Specifically, a reduction in the electric length of the L_2 parameter leads to an elevation in the resonant frequencies at the first and fourth modes.

Subsequently, during the investigation of the impact of $|S_{11}|$ with variations in the L_4 parameter, as seen in Fig. 3, it was observed that a rise in the L_4 parameter resulted in a downward shift of the second resonance frequency. There were no substantial alterations made to the first and third resonance frequencies.

However, the impedance bandwidth of the fourth resonance frequency deteriorates as the L_4 parameter increases. Based on the aforementioned findings, it is evident that augmenting the L_4 parameter leads to a rise in the electrical length, thus causing a significant reduction in the second resonance frequency. At the fourth resonance frequency, there is an observed rise in the mismatch impedance, resulting in a notable drop in the impedance bandwidth.

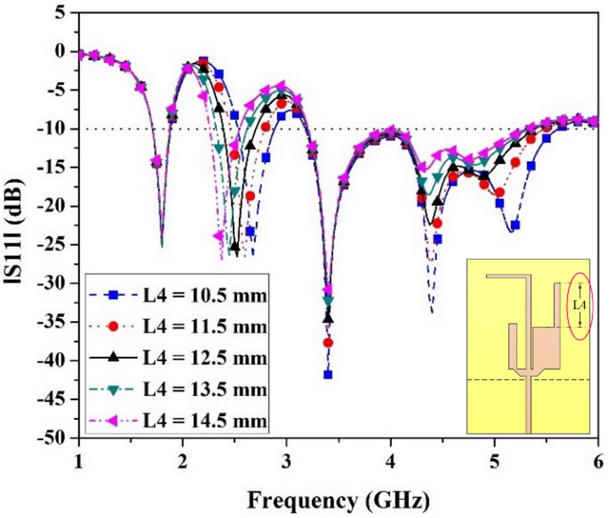

***Fig. 3**: The simulation result of the $|S_{11}|$ as varying the parameter L_4.*

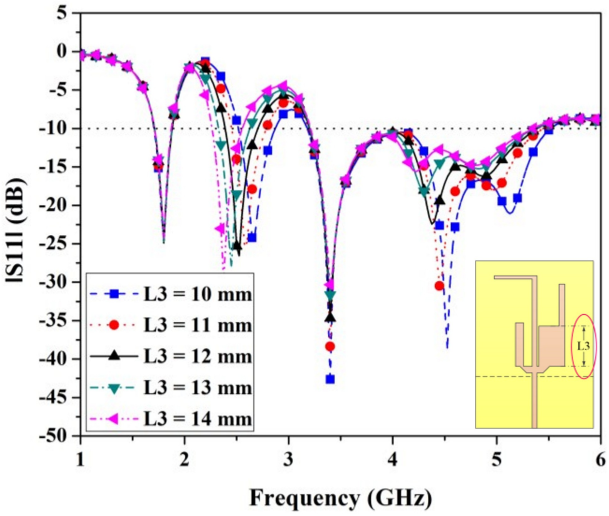

***Fig. 5**: The simulation result of the $|S_{11}|$ as varying the parameter L_3.*

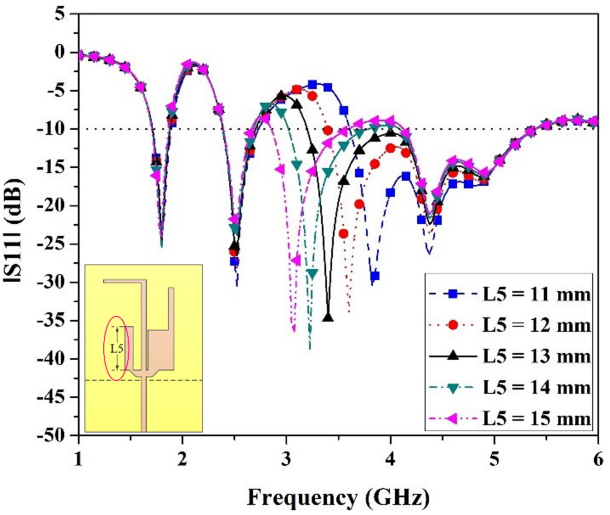

***Fig. 4**: The simulation result of the $|S_{11}|$ as varying the parameter L_5.*

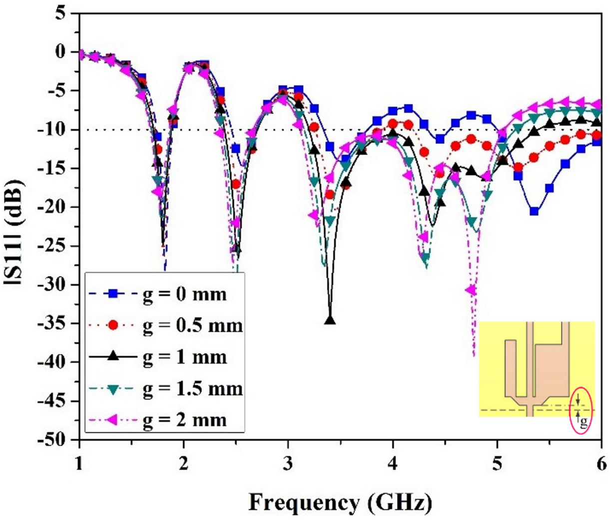

***Fig. 6**: The simulation result of the $|S_{11}|$ as varying the parameter g.*

Additionally, as seen in Fig. 4, the augmentation of the L_5 parameter value leads to a drop in the third resonance frequency. This phenomenon may be attributed to the concurrent rise in electrical length while the remaining resonant frequencies exhibited little changes. The findings demonstrate that the L_5 parameter has a high degree of autonomy in effectively regulating the third resonant frequency. Moreover, it is a parameter of notable significance in the generation of the third resonance frequency.

Fig. 5 illustrates the variation in the L_3 parameter. The augmentation of the L_3 parameter leads to a reduction in the resonant frequencies at the second and fourth modes, owing to the corresponding rise in the electrical length. The first and third resonance frequencies remain unaltered. However, it is evident that these actions not only induce a downward change in the resonance frequency. Furthermore, the fourth resonant frequency is likewise associated with a decrease in the impedance bandwidth.

Upon closer analysis of Fig. 6, it becomes evident that the manipulation of the crucial g parameter has a notable impact on the impedance bandwidth at the third and fourth resonant frequencies, leading to substantial fluctuations. The impact of the first and second resonant frequencies on the impedance bandwidth is minimal. The findings indicate that the g parameter has a significant influence on the impedance matching of the antenna under consideration.

2.2 Current Distribution Analysis

This section presents an analysis of the current distribution of the proposed antenna within the resonant

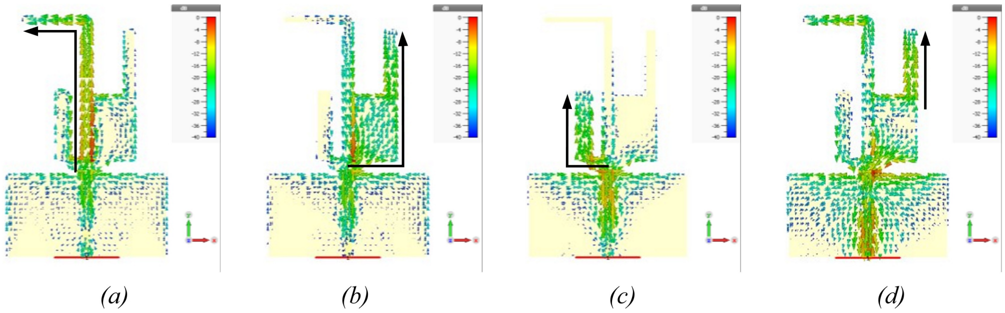

Fig. 7: Current distribution analysis of the proposed antenna at the resonant frequencies of (a) 1.8 GHz (b) 2.45 GHz (c) 3.6 GHz and (d) 5.25 GHz.

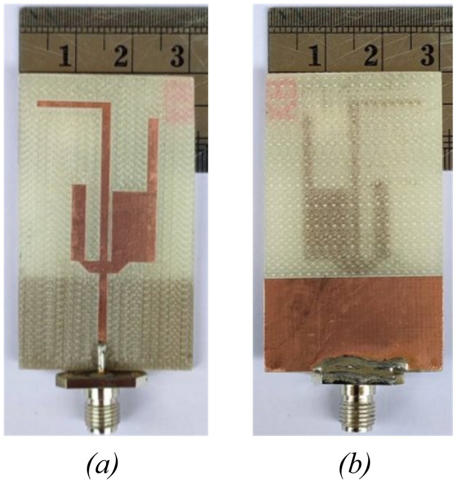

Fig. 8: The proposed antenna prototype (a) Top layer and (b) Bottom layer.

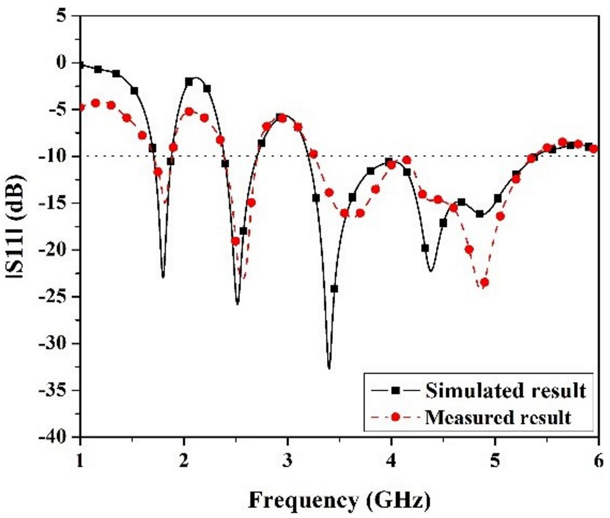

Fig. 9: The comparison between the simulated and measured results of the reflection coefficient $|S_{11}|$.

frequency ranges of 1.8 GHz, 2.45 GHz, 3.6 GHz, and 5.25 GHz. The objective is to identify the specific regions of the antenna that are influenced by the resonance frequency at various intended frequencies.

The examination of the antenna's current distribution may be ascertained by the use of the CST simulation software. By modeling the current distribution at a frequency of 1.8 GHz, as seen in Fig. 7(a), it is observed that a substantial portion of the current is concentrated in the L_1 and L_2 regions of the proposed antenna. The findings align with the examination of the impact of parameters discussed in the preceding section.

Subsequent analysis of the current distribution at a frequency of 2.45 GHz, as depicted in Fig. 7(b), revealed that the predominant flow of current around the antenna was concentrated within the regions defined by parameters L_3 and L_4. This observation suggests that parameters L_3 and L_4 exert a substantial influence on the resonance frequency at 2.45 GHz.

During the examination of the current distribution outcomes at a frequency of 3.6 GHz, as shown in Figure 7(c), it becomes evident that the current will traverse via the branch of the monopole antenna including the L_5 parameter region. The resonance frequency of the L_5 region is clearly seen to be 3.6 GHz. Consequently, independent control over the resonance frequency at 3.6 GHz may be achieved.

Furthermore, upon examination of the current distribution at a frequency of 5.25 GHz, as depicted in Fig. 7(d), it was observed that there exists a current distribution along the branch of the monopole antenna characterized by parameters L_2, L_3 and L_4. This observation suggests that the resonance at this particular frequency is attributed to the resonance of parameters L_2 and L_4, consequently resulting in a resonant frequency of 5.25 GHz. The manipulation of parameters L_2, L_3 and L_4 has been seen to have an impact on the regulation of this phenomenon, as previously discussed in relation to the alteration of parameter frequency.

Therefore, based on the examination of the existing distribution on the suggested antenna, it can be inferred that the frequency shift at the resonance frequency of 1.8 GHz can be regulated by adjusting the parameters L_1 and L_2. Similarly, at the resonance frequency of 2.45 GHz, the frequency shift can be effectively controlled by modifying the parameters L_3 and L_4. Specifically, the resonance frequency of 3.6 GHz may be changed independently by parameter L_5 without any impact

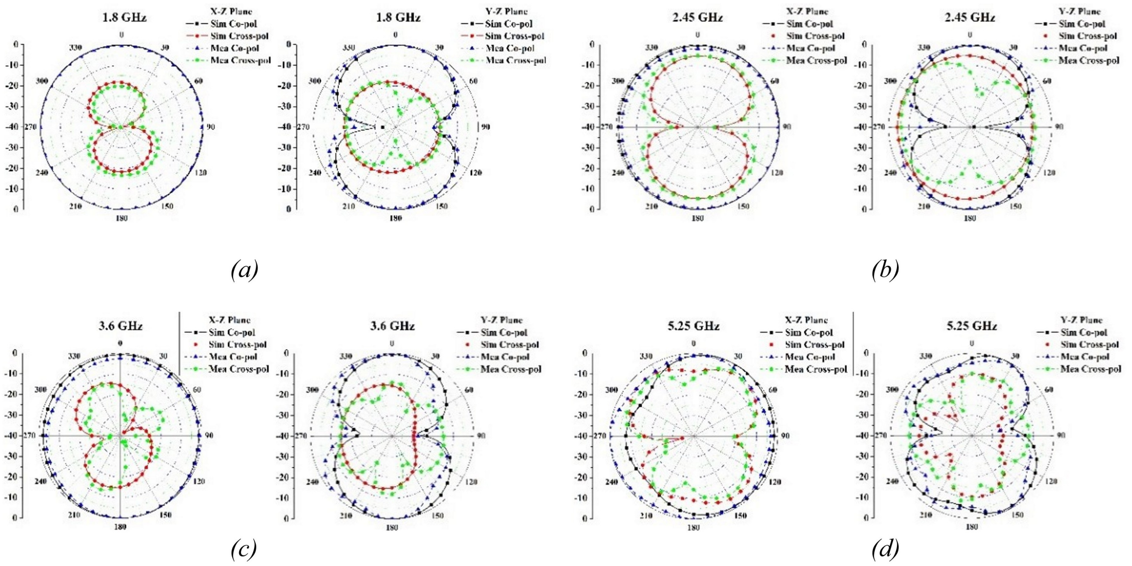

***Fig. 10**: he comparison between the simulated and measured results of the radiation pattern in X-Z planes and Y-Z planes at (a) 1.8 GHz (b) 2.45 GHz (c) 3.6 GHz and (d) 5.25 GHz.*

on other parameters. The modification of resonant frequency at 5.25 GHz is shown to have a substantial impact on the frequency modulation based on the L_2, L_3, and L_4 parameters.

Based on the simulation results obtained using CST simulation software, it was determined that the previously established antenna exhibits responsiveness throughout the frequency range of 1.8 GHz (1.71-1.89 GHz), 2.45 GHz (2.39-2.71 GHz), and 3.6 GHz (3.2-5.37 GHz). The following part will elucidate the comparison between the outcomes obtained from the simulation and the measurements. The article explores a range of antenna characteristics, including the reflection coefficient $|S_{11}|$, antenna gain, and radiation pattern. Additionally, the proposed antenna demonstrates efficiencies of 90.42%, 88.95%, 88.33%, and 76.88% at the center operating frequencies of 1.8 GHz, 2.45 GHz, 3.5 GHz, and 5.25 GHz, respectively.

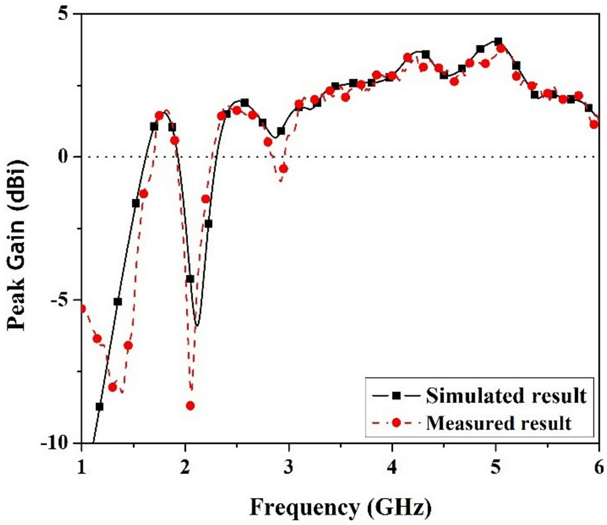

***Fig. 11**: The comparison of the proposed antenna's peak gain in both simulated and measured results.*

3. RESULTS AND DISCUSSIONS

This section presents the findings of a comparative analysis performed on different antenna properties derived from both simulation and measurement techniques. The antenna parameters in Table 1 were developed and implemented as a prototype using an LPKF etching machine. The material used in the fabrication of this piece was a readily accessible FR4 printed circuit board, which is widely available in the market and is cost-effective. Upon fabrication, it was determined that the dimensions of the antenna were 30×50 mm^2, with an SMA port affixed to the terminal of the microstrip transmission line. The schematic representation of the prototype is seen in Figure 8.

Subsequently, the antenna underwent measurement testing using a network analyzer, revealing its ability to cover resonant frequencies within the ranges of 1.8 GHz (1.71-1.89 GHz), 2.45 GHz (2.39-2.71), and 3.6 GHz (3.2-5.37 GHz). As seen in Fig. 9, however, based on the aforementioned findings, a comparison between the measurement findings and the simulation results revealed a strong agreement between the two. The device encompasses the resonant frequency bands of 1.8 GHz, 2.45 GHz, 3.6 GHz, and 5.25 GHz, exhibiting $|S_{11}|$ magnitudes below -10 dB within the designated frequency range of operation.

Subsequently, following the use of the prototype antenna for the purpose of assessing the radiation pattern inside the anechoic chamber, the resulting radiation pattern will be visually shown in the X-Z and Y-Z planes,

Table 2: *Performance comparison between the proposed antenna and the previous literature.*

Ref.	Dimension (mm.), (Volume) (mm^3)	Substrate (ε_r)	Freq. Band (GHz), (%BW)	Polarization	Radiation pattern	Average Gain (dBi)
[30]	35×50×0.8, (1,400)	FR4 (4.3)	2.26-2.62 (14.78%), 3.23-3.72 (14.35%), 4.36-7.96 (51.95%)	Linear	Omnidirectional	2.0
[31]	50×50×1, (2,500)	FR4 (4.4)	1.71-3.66 (72..63%)	Linear	Omnidirectional	2.5
[32]	30×40×1.6 (1,920)	FR4 (4.4)	1.81-1.98 (8.95%), 2.4-2.83 (16.54%), 3.3-3.73 (12.11%), 5.0-5.94 (17.25%),	Linear	Omnidirectional	1.4
[33]	60×70×31.6 (132,720)	FR4 (4.4)	1.68-1.91 (12.71%), 2.36-2.5 (5.74)	Linear	Unidirectional	5.0
[34]	47×67×1 (3149)	FR4 (4.4)	1.5-6.0 (120%)	Linear	Omnidirectional	2.5
[35]	38×77×1.6 (4,681.6)	FR4 (4.1)	1.62-1.90 (15.55%), 2.31-2.52 (8.75%), 3.23-4.38 (31.94%)	Linear	Omnidirectional	1.5
[36]	96×64.2×11.5 (70,876.8)	FR4 (4.3)	1.62-2.78 (52.7%)	Linear	Unidirectional	5.0
Proposed Ant.	30×50×0.8 (1,200)	FR4 (4.3)	1.71-1.89 (10.00%), 2.39-2.71 (12.70%), 3.20-5.37 (50.64),	Linear	Omnidirectional	2.5

as illustrated in Fig. 10. Based on the findings, it was noted that the radiation pattern had omnidirectional properties at frequencies of 1.8 GHz, 2.45 GHz and 3.6 GHz, as seen in Fig. 10. Nevertheless, it is observed that the level of cross-polarization radiation pattern shown by the antenna tends to rise as the frequency rises. At the frequency of 5.25 GHz, it is evident that the radiation pattern deviates from the typical omnidirectional pattern, exhibiting distortion. Additionally, the higher-order mode of the antenna introduces further distortion in the form of a cross-polarization radiation pattern. Based on the findings, the observed outcomes align with the examination of the current distribution on the proposed antenna at a frequency of 5.25 GHz, which may be attributed to the presence of the third harmonic frequency of parameter L_2 and the second harmonic frequency of parameter L_3 and L_4.

Upon measurement of the proposed antenna, it was determined that the maximum gain of the antenna, a significant attribute, was approximately 2.2 dBi at frequencies of 1.8 GHz and 2.45 GHz. Additionally, the antenna exhibited gains of approximately 2.7 dBi and 3 dBi at frequencies of 3.6 GHz and 5.25 GHz, respectively, as depicted in Fig. 11. The aforementioned findings demonstrate a strong concurrence between the simulated antenna gain and the measured antenna gain.

4. CONCLUSIONS

This research demonstrates the incorporation of a triple L-shaped structure onto a monopole antenna to enable its functioning over many frequency bands. The antenna under consideration can efficiently function across the frequency ranges of 1.8 GHz (1.71−1.89 GHz), 2.45 GHz (2.39−2.71), and 3.6 GHz (3.2−5.37 GHz), which are commonly utilized for Wireless Local Area Network (WLAN), Worldwide Interoperability of Microwave Access (WiMAX), and 5G networks. The antenna design consists of three components in the shape of the letter L. The resonant frequencies may vary among L-shaped structures.

The investigation found that the middle L-shaped structure demonstrates resonance at the frequencies corresponding to the first and fourth. Similarly, the right L-shaped structure exhibits good responsiveness at the second and fourth resonant frequencies. In addition, the L-shaped structure on the left demonstrates autonomous responsiveness and control over the third resonant frequency without requiring any additional structural components. However, the antenna being discussed adequately covers the specified operating frequencies, showing a reflection coefficient of S_{11} levels below -10 dB across the whole frequency range.

In addition, the antenna's radiation pattern displays omnidirectional properties at the resonant frequencies of 1.8 GHz, 2.45 GHz, and 3.6 GHz. However, the antenna's radiation pattern at 5.25 GHz exhibits significant distortion as a result of the presence of higher-order modes, which affects the radiation pattern's overall form.

Among other discoveries, it was ascertained that the antenna demonstrated an average gain of around 2.5 dBi across its entire range of operational frequencies. Additionally, the antenna being discussed is fabricated utilizing FR4-printed circuit boards, which offer the benefits of cost-effectiveness, easy availability, and durability. The antenna mentioned in this context is smaller and more streamlined compared to the study mentioned in Table 2. The antenna has dimensions of 30×50 mm^2. Therefore, the antenna described in this document is considered suitable for implementation in small wireless communication devices that function as both Wi-Fi signal boosters and effectively connect to the 4G and 5G cellular networks.

ACKNOWLEDGEMENT

This research block grant was managed under Rajamangala University of Technology Thanyaburi (FRB66E2801). Additionally, this research was funded by National Science, Research, and Innovation Fund (NSRF), and King Mongkut's University of Technology North Bangkok with Contract no. KMUTNB-FF-67-B-16.

REFERENCES

[1] Y. Feng, J.-Y. Li, L.-K. Zhang, X.-J. Yu, Y.-X. Qi, D. Li and S.-G. Zhou, "A Broadband Wide-Angle Scanning Linear Array Antenna with Suppressed Mutual Coupling for 5G Sub-6G Applications," *IEEE Antennas and Wireless Propagation Letters*, vol. 21, no. 2, pp. 366-370, 2022.

[2] X. Tang, H. Chen, B. Yu, W. Che and Q. Xue, "Bandwidth Enhancement of a Compact Dual-Polarized Antenna for Sub-6G 5G CPE," *IEEE Antennas and Wireless Propagation Letters*, vol. 21, no. 10, pp. 2015-2019, 2022.

[3] W. Chanwattanapong, N. Wongsin, P. Rakluea, T. Jangjing, T. Suangun, W. Thaiwirot and C. Mahatthanajatuphat, "Dualband Cross Bowtie Dipole for 5G Base Station Antenna" *Proceeding of 19th International Conference on Electrical Engineering/Electronics, Computer, Telecommunications and Information Technology (ECTI-CON 2022)*, pp. 1-4, 2022.

[4] Y. Feng, L.-K. Zhang, J.-Y. Li, Y.-H. Yang, S.-G. Zhou and X.-J. Yu, "A Compact Share-Aperture Antenna with Pattern/Polarization Diversity for 5G Sub-6G Applications," *IEEE Transactions on Circuits and Systems II: Express Briefs,* vol. 70, no. 3, pp. 954-958, 2023.

[5] Y.-C. Zhao, I-F. Chen, C.-M. Peng and ¹L. Gao, "Ten-port Sub-6G Antenna for 5G Smartphone Applications" *Proceeding of 9th Asia-Pacific Conference on Antennas and Propagation (APCAP 2020)*, pp. 1-2, 2020.

[6] F. Ahmed, M. H. M. Chowdhury and N. Hasan, "A Compact Multiband Antenna for 4G/LTE and WLAN Mobile Phone Applications" *Proceeding of 3th International Conference on Electrical Engineering and Information & Communication Technology (ICEEICT 2016)*, pp. 1-4, 2016.

[7] A. Nella and A. S. Gandhi, "A Survey on Microstrip Antennas for Portable Wireless Communication System Applications" *Proceeding of International Conference on Advances in Computing, Communications and Informatics (ICACCI 2017)*, pp. 2156-2165, 2017.

[8] C.-J. Lee, K. M. K. H. Leong and T. Itoh, "Broadband Small Antenna for Portable Wireless Application" *Proceeding of International Workshop on Antenna Technology: Small Antennas and Novel Metamaterials (IWAT 2008)*, pp. 10-13, 2008.

[9] N. Wongsin, T. Suangun, C. Mahatthanajatuphat and P. Akkaraekthalin, "A rhombic ring monopole antenna with stripline and ring resonator for multiband operation" *Proceeding of 14th International Conference on Electrical Engineering/Electronics, Computer, Telecommunications and Information Technology (ECTI-CON 2017)*, pp. 706-709, 2017.

[10] J.-W. Kim, T.-H. Jung, H.-K. Ryu, J.-M. Woo, C.-S. Eun and D.-K. Lee, "Compact Multiband Microstrip Antenna Using Inverted-L- and T-Shaped Parasitic Elements," *IEEE Antennas and Wireless Propagation Letters*, vol. 12, pp. 1299-1302, 2013.

[11] S. Shoaib, I. Shoaib, N. Shoaib, X. Chen and C. G. Parini, "Design and Performance Study of a Dual-Element Multiband Printed Monopole Antenna Array for MIMO Terminals," *IEEE Antennas and Wireless Propagation Letters*, vol. 13, pp. 329-332, 2014.

[12] M. Borhani, P. Rezaei and A. Valizade, "Design of a Reconfigurable Miniaturized Microstrip Antenna for Switchable Multiband Systems," *IEEE Antennas and Wireless Propagation Letters*, vol. 15, pp. 822-825, 2016.

[13] C.-J. Lee, K. M. K. H. Leong and T. Itoh, "High Gain Multiband Circular Loop Antenna with Ring Resonators Reflectors by using FSS Technique" *Proceeding of International Workshop on Antenna Technology: Small Antennas and Novel Metamaterials (IWAT 2015)*, pp. 338-341, 2015.

[14] J. Cui, A. Zhang and X. Chen, "An Omnidirectional Multiband Antenna for Railway Application," *IEEE Antennas and Wireless Propagation Letters*, vol. 19, no. 1, pp. 54-58, 2020.

[15] S. Jayant and G. Srivastava, "Close-Packed Quad-Element Triple-Band-Notched UWB MIMO Antenna with Upgrading Capability," *IEEE Transactions on Antennas and Propagation*, vol. 71, no. 1, pp. 353-360, 2023.

[16] M. Rahman, A. Haider and M. Naghshvarian-jahromi, "A Systematic Methodology for the Time-Domain Ringing Reduction in UWB Band-Notched Antennas" *IEEE Antennas and Wireless Propagation Letters*, vol. 19, no. 3, pp. 482-486, 2020.

[17] S. Jayant, G. Srivastava and M. Khari, "8-Port MIMO Antenna Having Two Notched Bands for Chipless UWB-RFID Tags," *IEEE Journal of Radio Frequency Identification*, vol. 6, pp. 355-360, 2022.

[18] Z. Zhao, C. Zhang, Z. Lu, H. Chu, S. Chen, M. Liu and G. Li, "A Miniaturized Wearable Antenna with Five Band-Notched Characteristics for Medical Applications," *IEEE Antennas and Wireless Propagation Letters*, vol. 22, no. 6, pp. 1246-1250,

2023.

[19] Z. Li, C. Yin and X. Zhu, "Compact UWB MIMO Vivaldi Antenna with Dual Band-Notched Characteristics," *IEEE Access*, vol. 7, pp. 38696-38701, 2019.

[20] S. Zhang, X.-S. Yang, B.-J. Chen and B.-Z. Wang, "Miniaturized Wideband ±45° Dual-Polarized Metasurface Antenna by Loading Quasi-Fractal Slot," *IEEE Antennas and Wireless Propagation Letters*, vol. 22, no. 4, pp. 893-897, 2023.

[21] C. Mahatthanajatuphat, T. Suangun, N. Wongsin, and P. Akkaraekthalin, "Triband Operation Enhancement Based on Multimode Analytics of Modified Rhombic Ring Structure with Fractal Ring Parasitic," *International Journal of Antennas and Propagation*, vol. 2019, pp. 1-10, 2019.

[22] C. Mahatthanajatuphat, S. Saleekaw, P. Akkaraekthalin, and M. Krairiksh, "A rhombic patch monopole antenna with modified Minkowski fractal geometry for UMTS, WLAN, and mobile WiMAX application," *Progress In Electromagnetics Research*, vol. 89, pp. 57-74, 2009.

[23] M. Kumar and V. Nath, "Multiband CPW-fed Circular Microstrip Antenna with Modified Cantor Fractal Slot for DCS/GPS/WiMAX/WLAN/HiPERLAN2 Applications" *Proceeding of International Conference on Wireless Communications, Signal Processing and Networking (WiSPNET 2018)*, pp. 1-5, 2018.

[24] Y. B. Chaouche, M. Nedil, B. Hammache and M. Belazzoug, "Design of Modified Sierpinski Gasket Fractal Antenna for Tri-band Applications" *Proceeding of 2019 IEEE International Symposium on Antennas and Propagation and USNC-URSI Radio Science Meeting*, pp. 889-890, 2019.

[25] X. Wang, Y. Wu, W. Wang and A. A. Kishk, "A Simple Multi-Broadband Planar Antenna for LTE/GSM/UMTS and WLAN/WiMAX Mobile Handset Applications," *IEEE Access,* vol. 6, pp. 74453-74461, 2018.

[26] K.-C. Lin, C.-H. Lin and Y.-C. Lin, "Simple Printed Multiband Antenna with Novel Parasitic-Element Design for Multistandard Mobile Phone Applications," *IEEE Transactions on Antennas and Propagation*, vol. 61, no.1, pp. 488-491, 2013.

[27] H. Huang, Y. Liu, S. Zhang and S. Gong, "Multiband Metamaterial-Loaded Monopole Antenna for WLAN/WiMAX Applications," *IEEE Antennas and Wireless Propagation Letters*, vol. 14, pp. 662-665, 2015.

[28] N. Wongsin, T. Suangun, C. Mahatthanajatuphat and P. Akkaraekthalin, "A Multiband Fractal Ring Antenna Fed by Capacitive Coupling" *Proceeding of 8th International Conference on Electrical Engineering/Electronics, Computer, Telecommunications and Information Technology (ECTI-CON 2011)*, pp. 204-207, 2011.

[29] A. K. Gautam, L. Kumar, B. K. Kanaujia and K. Rambabu, "Design of Compact F-Shaped Slot Triple-Band Antenna for WLAN/WiMAX Applications," *IEEE Transactions on Antennas and Propagation*, vol. 64, no. 3, pp. 1101-1105, 2016.

[30] M. Tangjitjetsada, T. Suangun, W. Chanwattanapong, C. Mahatthanajatuphat, K. Phimthai and P. Akkaraekthalin, "A Multiband Tri-branch Monopole Antenna Base on Step Impedance Technique for WLAN, WiMAX, 5G Technology, and IoT Application" *Proceeding of 20th International Conference on Electrical Engineering/Electronics, Computer, Telecommunications and Information Technology (ECTI-CON 2023)*, pp. 1-4, 2023.

[31] Z.-J. Jin and T.-Y. Yun, "Compact Wideband Open-End Slot Antenna with Inherent Matching," *IEEE Antennas and Wireless Propagation Letters,* vol. 13, pp. 1385-1388, 2014.

[32] A. Dadgarpour, A. Abbosh and F. Jolani, "Planar Multiband Antenna for Compact Mobile Transceivers," *IEEE Antennas and Wireless Propagation Letters*, vol. 10, pp.651-654, 2011.

[33] A. Raveendran and S. Raman, "Dual-band Antennas with Multifunctional Beam for DCS/WLAN Applications" *Proceeding of 2018 IEEE Indian Conference on Antennas and Propogation (InCAP 2018)*, pp. 1-4, 2018.

[34] R. Eshtiaghi, M. G. Shayesteh and N. Zad-Shakooian, "Multicircular Monopole Antenna for Multiband Applications," IEEE Antennas and Wireless Propagation Letters, vol. 10, pp.1205-1207, 2011.

[35] C. Mahatthanajatuphat, N. Wongsin and P. Akkaraekthalin, "A Multiband Monopole Antenna with Modified Fractal Loop Parasitic for DCS 1800, WLAN, WiMAX and IMT Advanced Systems," *IEICE Transactions on Communications*, vol. E95-B, no. 1, pp. 27-33, 2012.

[36] W. An, X. Wang, H. Fu, J. Ma, X. Huang and B. Feng, "Low-Profile Wideband Slot-Loaded Patch Antenna with Multiresonant Modes," *IEEE Antennas and Wireless Propagation Letters*, vol. 17, no.7, pp. 1309-1313, 2018.

Vanvisa Chutchavong received the B.Ind.Tech. degree in electronics technology, M.Eng. degree in information engineering, and D.Eng degree in electrical engineering from the King Mongkut's Institute of Technology Ladkrabang (KMITL), Thailand, in 2000, 2003, and 2011, respectively. Since 2005, she has been with King Mongkut's Institute of Technology Ladkrabang (KMITL), Thailand, where she is recently an Assistant Professor. Also, she is a Lecturer. Her current research interests include image/signal processing, filter design, Smart IoT, railway technology and signalling.

Wanchalerm Chanwattapong received the B.Eng. degree in electrical engineering from Khon Kaen University, M.Eng. degree in information engineering, from the King Mongkut's Institute of Technology Ladkrabang (KMITL), Thailand, in 2001 and 2007. Since 2010, he has worked as a lecturer in Rajamangala University of Technology Thanyaburi (RMUTT), Thailand. His current research interests include IoT, machine learning, and thin-film antenna.

Thinnawat Jangjing received the B.Eng degree in Electronics and Telecommunication Engineering and an M.Eng degree in Electrical Engineering (Telecommunication) from Rajamangala University of Technology Thanyaburi (RMUTT), Thailand, in 2009 and 2012, respectively. He has been a lecturer at Faculty of Engineering, Rajamangala University of Technology Thanyaburi (RMUTT), Thailand. His research interests include renewable energy, wearable antenna IoT, and LoRA applications.

Paitoon Rakluea received the B.Ind.Tech. degree in electronics technology, M.Eng. degree in information engineering, and D.Eng degree in electrical engineering from the King Mongkut's Institute of Technology Ladkrabang (KMITL), Thailand, in 2000, 2003, and 2009, respectively. Since 2003, he has been with Rajamangala University of Technology Thanyaburi (RMUTT), Thailand, where he is recently an Assistant Professor. Also, he is a Lecturer and the Head of the Department of Electronics and Telecommunication Engineering. His current research interests include signal processing, RF/microwave circuits, wideband and multiband antennas, wearable antenna, and thin-film antenna.

Norakamon Wongsin received B.Eng., M.Eng. and Ph.D. degrees in Electrical Engineering from King Mongkut's University of Technology North Bangkok (KMUTNB), Thailand, in 2009, 2012 and 2019, respectively. Since 2012, he has been a lecturer at Department of Electronics and Telecommunication Engineering, Faculty of Engineering, Rajamangala University of Technology Thanyaburi (RMUTT), Thailand. His research interests include wideband and multiband small antennas for communication applications.

Thanakarn Suangunreceived B.Eng., M.Eng. and Ph.D. degrees in Electrical Engineering from King Mongkut's University of Technology North Bangkok (KMUTNB), Thailand, in 2006, 2009 and 2020, respectively. Since 2012, he has been a lecturer at Department of Electrical Engineering, School of Engineering, University of Phayao, Thailand. His research interests include RF/Microwave, multiband small antennas for communication applications and Automation.

Chatree Mahatthanajatuphat received the M.Eng. degree from the University of Applied Sciences Rosenheim, Germany, in 2003, and the Ph.D. degree from the King Mongkut's University of Technology North Bangkok (KMUTNB), Thailand, in 2009. In 2017, he was appointed as a Lecturer (Associate Professor) at the Department of Electrical Engineering, KMUTNB, as a Lecturer. His main research interests include the designing of small antennas using the fractal geometry concept and digital signal processing for communication applications.

Nonchanutt Chudpooti received the B.Sc. degree (Hons.) in industrial physics and medical instrumentation and the Ph.D. degree in electrical engineering from the King Mongkut's University of Technology North Bangkok, in 2012 and 2018, respectively, where he was appointed as a Lecturer at the Department of Industrial Physics and Medical Instrumentation, Faculty of Applied Science, in 2018. His main research interests include the application of microwave microfluidic sensors, millimeter-wave substrate integrated circuit applications, and substrate integrated waveguide applications. He was a recipient of the Best Presentation Award from the Thailand-Japan Microwave, in 2015 and 2018, and the Young Researcher Encouragement Award, in 2016.

Prayoot Akkaraekthalin He received the B.Eng. and M.Eng. degrees in Electrical Engineering from King Mongkut's University of Technology North Bangkok (KMUTNB), Thailand, in 1986 and 1990, respectively, and the Ph.D. degree from the University of Delaware, Newark, USA, in 1998. From 1986 to 1988, he worked in the Microtek Laboratory, Thailand. In 1988, he joined the Department of Electrical Engineering, KMUTNB. His current research interests include passive and active microwave circuits, wideband and multiband antennas, and telecommunication systems. Dr. Prayoot is members of IEEE, IEICE Japan, and ECTI Thailand. He was the Chairman for the IEEE MTT/AP/ED Thailand Joint Chapter during 2007 and 2008 and the President of ECTI Association from 2014 to 2015. He is now the head for Senior Research Scholar Project of Thailand Research Fund (TRF).